STARS

The Pegasus Review: UCF Undergraduate Research Journal

Volume 13 | Issue 1 Article 2

2021

A Jones Calculus Approach to High-Order Harmonic Generation in Solids

Erin Crites
University of Central Florida, ecrites@knights.ucf.edu

Shima Gholam-Mirzaei
University of Central Florida, shmirzaei@knights.ucf.edu

Zain Khan
University of Central Florida, xainulabedin@knights.ucf.edu

Mamta Singh
University of Central Florida, mamta@knights.ucf.edu

John E. Beetar
University of Central Florida, oneironaut@knights.ucf.edu

 Part of the Physics Commons

Find similar works at: https://stars.library.ucf.edu/urj
University of Central Florida Libraries http://library.ucf.edu

This Article is brought to you for free and open access by the Office of Undergraduate Research at STARS. It has been accepted for inclusion in The Pegasus Review: UCF Undergraduate Research Journal by an authorized editor of STARS. For more information, please contact STARS@ucf.edu.

Recommended Citation

Crites, Erin; Gholam-Mirzaei, Shima; Khan, Zain; Singh, Mamta; and Beetar, John E. (2021) "A Jones Calculus Approach to High-Order Harmonic Generation in Solids," *The Pegasus Review: UCF Undergraduate Research Journal*: Vol. 13 : Iss. 1 , Article 2.
Available at: https://stars.library.ucf.edu/urj/vol13/iss1/2

A Jones Calculus Approach to High-Order Harmonic Generation in Solids

Cover Page Footnote

Please note that the following work was submitted August 2019 and is part of a larger work entitled “Polarization Dependence of High Order Harmonic Generation from Solids in Reflection and Transmission Geometries” that was published through the UCF BHC Honors in the Major program in May of 2020.

This article is available in The Pegasus Review: UCF Undergraduate Research Journal: https://stars.library.ucf.edu/urj/vol13/iss1/2

Vol. 13.1: 11-19

URJ

THE PEGASUS REVIEW:
UNIVERSITY OF CENTRAL FLORIDA
UNDERGRADUATE RESEARCH JOURNAL

Published
February 22nd, 2021

A Jones Calculus Approach to High-Order Harmonic Generation in Solids

By: Erin Crites, Shima Gholam-Mirzaei, Zain Khan, Mamta Singh, and John E. Beetar

Faculty Mentor: Dr. Michael Chini

UCF Department of Physics

ABSTRACT: High-order harmonics from bulk solids were first observed in 2011 by focusing an intense mid-infrared laser through a bulk crystal and detecting the harmonics in a transmission geometry. Due to birefringence and possible nonlinear effects in bulk crystal, the polarization state of the laser can change as it propagates through the crystal in this transmission geometry. This can result in harmonic signal generated with an unknown polarization of light, disrupting the signal. Alternatives to bulk crystal, such as a reflection geometry or thin films, are not always ideal – reflection geometry can introduce nonlinear reflection coefficients, while crystalline thin films can be difficult to produce and are not available for all materials. We propose Jones calculus as a new method to analyze high-order harmonics from bulk solids in a transmission geometry. We predict the laser's polarization changes due to propagation through a bulk crystal and we show that these changes can be accounted for using a combination of wave plates. Our results indicate that linear birefringence dominates the polarization change in bulk ZnO crystals driven in the mid-IR, which allows us to neglect the effect of nonlinear propagation effects on the polarization state. After compensating for the birefringence, we observe ellipticity-dependent, rotationally sensitive features in the harmonic signal which differ from those observed in previous transmission-geometry experiments. This method increases confidence in and control of HHG measurements in bulk crystal.

KEYWORDS: Jones calculus; ultrafast lasers; nonlinear optics; high-order harmonic generation; ZnO

Republication not permitted without written consent of the author.

THE PEGASUS REVIEW:
UNIVERSITY OF CENTRAL FLORIDA
UNDERGRADUATE RESEARCH JOURNAL

URJ

13.1: 11-19

INTRODUCTION

High-order harmonic generation (HHG) in gases is a powerful tool for studying atomic and molecular structure and dynamics[1-4] through the development of high-order harmonic spectroscopy[5-7]. With the recent development of HHG in solids[8], there is potential to extend high-order harmonic spectroscopy to problems in condensed matter physics, such as reconstruction of the electronic band structure[9] and studies of quasiparticle dynamics[10]. Bridging the gap from gas- to solid-phase systems requires an understanding of the underlying mechanisms of HHG in these systems, including the effects from the propagation of the laser and the harmonic generation process.

HHG is a recollisional process in which electrons and holes excited by tunneling are accelerated within the conduction and valence bands and emit coherent high frequency light upon recombination. In solids, the HHG process most significantly occurs in the last layers of the crystals, as the harmonic signal is absorbed during propagation through the crystal[11]. Many factors affect harmonic signal. The symmetry of the system, and by extension, different crystal structures and orientations, affects the harmonic signal strength. Laser polarization can also result in different signals, creating the need for angle-dependent measurements[12, 13]. The ellipticity of the driving laser also affects the harmonic signal, where large ellipticities greatly impact harmonic signal in gases[14] and thus have been used as a gating mechanism[15, 16]. In contrast, large ellipticities can be used to generate circularly polarized harmonics in solids[17, 18]. Ellipticity affects interband and intraband harmonic contributions differently, resulting in signals dependent on the harmonic order and ellipticity of the input laser light[19, 20]

Due to the birefringent nature of many nonlinear crystals used in HHG, a linear laser polarization sent into a bulk crystal does not remain linear during propagation through the crystal. Rather, the polarization can develop a phase delay associated with the thickness of the crystal and the difference between the two indices of refraction. Because the HHG process occurs in the last layers of the crystal[8], the polarization may no longer be linear at the location of harmonic generation, altering the harmonic signal in an unknown capacity. Alternatives to bulk crystal are not always ideal or possible. For example, a reflection geometry[21, 22] with harmonics generated on the front surface of the crystal and reflecting off will not have the propagation effects seen in bulk crystal. Instead, this setup may result in nonlinear reflection coefficients and diminished power for high-order harmonics[21]. HHG in thin films[19] minimizes propagation effects related to the thickness of the crystal, but thin films are not available for all compounds and, when available, can be expensive, with long lead times.

To increase confidence in bulk crystal measurements, we propose Jones calculus analysis to model the optical system and determine the effect of the nonlinear crystal on the polarization. This analysis will allow us to control and more accurately analyze harmonic signal. With this method, the polarization at the location of the HHG can be characterized and controlled, opening up new possibilities in the applications of bulk crystals.

METHODS

In Jones calculus, a 2x2 matrix describes how an optic affects the polarization of light, represented by a vector. With simple matrix multiplication, an entire optical system can be written as a single matrix that describes the total effect on polarization of light traveling through the system[23]. The output polarization state of a system can be found by multiplying an input polarization vector by the effective matrix of the system.

We used ZnO, which is among the most commonly-used crystals for solid-state HHG, and modeled this nonlinear, birefringent crystal as an arbitrary wave plate[23], where $\theta_{crystal}$ is the angle of the crystal axis.

$$J_{crystal} = \begin{bmatrix} cos^2\,\theta_{crystal} + e^{i\,\Delta\phi}\,sin^2\,\theta_{crystal} & \left(1 - e^{i\,\Delta\phi}\right) sin\,\theta_{crystal}\,cos\,\theta_{crystal} \\ \left(1 - e^{i\,\Delta\phi}\right) sin\,\theta_{crystal}\,cos\,\theta_{crystal} & sin^2\,\theta_{crystal} + e^{i\,\Delta\phi}\,cos^2\,\theta_{crystal} \end{bmatrix} \quad (1)$$

THE PEGASUS REVIEW:
UNIVERSITY OF CENTRAL FLORIDA
UNDERGRADUATE RESEARCH JOURNAL

URJ

13.1: 11-19

The polarization phase delay caused by the difference between the ordinary and extraordinary indices is contained in the $\Delta\phi$ factor, where

$$\Delta\phi = \frac{2\pi d}{\lambda}\left(n_{extraordinary} - n_{ordinary}\right), \quad (2)$$

contains the dependence on the physical features of the experiment, such as the wavelength, the crystal's thickness, and the crystal's ordinary and extraordinary refractive indices.

To counteract the elliptically polarized light from the crystal, the setup also requires a half-wave plate (HWP) and quarter-wave plate (QWP). A HWP rotates linearly polarized light and occurs when the phase delay between the ordinary and extraordinary axis of a birefringent material is

$$\Delta\phi = \pi \pm 2m\pi \quad (3)$$

where m is an arbitrary integer. This simplifies *Equation (1)* into the Jones matrix for a HWP:

$$J_{HWP} = \begin{bmatrix} cos(2\theta_{HWP}) & sin(2\theta_{HWP}) \\ sin(2\theta_{HWP}) & -cos(2\theta_{HWP}) \end{bmatrix} \quad (4)$$

With a similar mathematical process, a QWP uses a birefringent material to convert linear polarization into circular polarization when the phase delay between ordinary and extraordinary axes is

$$\Delta\phi = \frac{\pi}{2} \pm 2m\pi. \quad (5)$$

forming the Jones matrix for a QWP

$$J_{QWP} = \begin{bmatrix} cos^2\theta_{QWP} + i\,sin^2\theta_{QWP} & (1-i)\,sin\theta_{QWP}\,cos\theta_{QWP} \\ (1-i)\,sin\theta_{QWP}\,cos\theta_{QWP} & sin^2\theta_{QWP} + i\,cos^2\theta_{QWP} \end{bmatrix} \quad (6)$$

to convert linear polarization into circular polarization. This mathematical representation of optical elements shows that all possible polarizations can be generated at the exit of the nonlinear crystal with the use of a HWP and QWP before the crystal.

Calculations were done in Python. An effective matrix was calculated for all possible angle combinations of the HWP, QWP, and ZnO. To replicate experimental conditions, we input a wavelength of 3400 nm, the corresponding indices of refraction of ZnO to that wavelength, a crystal thickness of 300 μm, and a vertical input polarization into the calculations. From this matrix, we used the polarization vector after passing through all possible configurations of the setup to calculate the ellipticity and angle of polarization of the output polarization. Angle combinations resulting in a small ellipticity (less than 0.0125) and vertical polarization were extracted for use in the experimental setup. There were often multiple possible angle combinations that resulted in similar ellipticities and polarization angles. For these cases, we chose angles that allowed for easiest setup transitions, but all combinations gave effectively equivalent results.

The results of the calculations were compared to experimental measurements of HHG in bulk ZnO crystals. The experiment was set up using the calculated angle values such that the laser passed through the half-wave plate and quarter-wave plate before focusing onto the back of the 300 μm thick ZnO crystal (Figure 1).

We used a commercial OPA (Light Conversion ORPHEUS-ONE) pumped by a 20 W Yb:KGW (Ytterbium-doped Potassium Gadolinium Tungstate) regenerative amplifier (Light Conversion PHAROS) at repetition rate of 50 kHz. The OPA idler output pulses (duration ~90 fs) at a wavelength of 3.4 μm, corresponding to the coatings on the half wave plate and quarter wave plate. The beam size was increased with a telescope (2.5x magnification), then passed through the half wave plate and quarter wave plate. An AR-coated Si lens was used to focus onto the back of the 300 μm thick ZnO crystal (University Wafer). The focal spot diameter was about 60 μm with a vacuum intensity of 0.6 TW/cm². All three optical elements were set at the desired angles using rotational mounts. Ellipticity measurements were taken with a power meter (Newport 843-R) and an absorptive polarizer. The generated harmonics were focused by an aluminum mirror onto a UV-enhanced high-resolution spectrometer (Ocean Optics HR2000+ES).

THE PEGASUS REVIEW:
UNIVERSITY OF CENTRAL FLORIDA
UNDERGRADUATE RESEARCH JOURNAL

URJ

13.1: 11-19

RESULTS AND DISCUSSION

First, we verified that the ZnO behaved as an arbitrary wave retarder, as described by the Jones matrix. We measured the polarization of the light after a vertical, linear polarization was passed through the ZnO crystal. Figure 2 shows the fraction of incident power transmitted through a polarizer for various orientations of the crystal compared to a calculation performed using the same crystal thickness and tabulated values for the ZnO refractive indices[24]. This figure shows the change from vertical input polarization due to only the ZnO crystal. A larger amplitude signifies smaller polarization ellipticity after passing through the ZnO, while a smaller amplitude signifies a larger polarization ellipticity, or that the light is closer to circular polarization. The ellipticity values are shown in Figure 3a. The experimental values follow the expected ellipticity values for different ZnO angles, where 45 degrees is the location of the most significant ellipticity change. The minima of the curve in Figure 2 were used to find the angle of polarization after the ZnO crystal (Figure 3b). The polarization angle varied a total of 40 degrees through the entire scan. The measured angle drifts from the calculated values around 0 or 90 degrees, which may be due to an insensitivity in the power measurements to small changes.

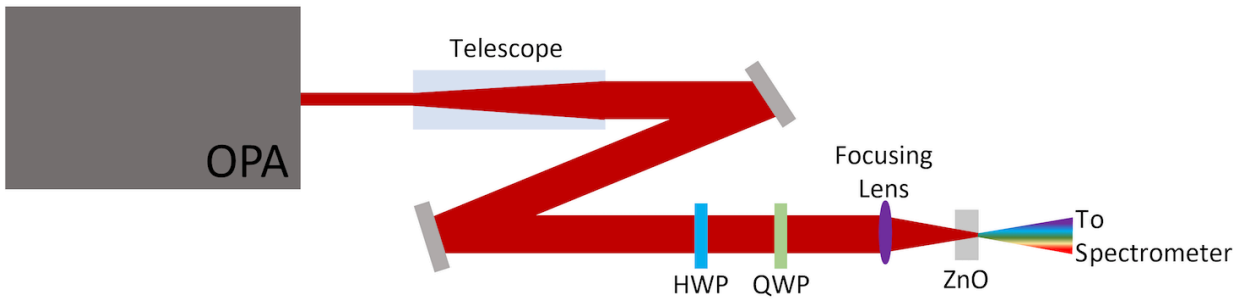

Figure 1. Experimental setup. The HHG process only significantly occurs at the exit plane of the crystal; which is the location at which the polarization should be linear.

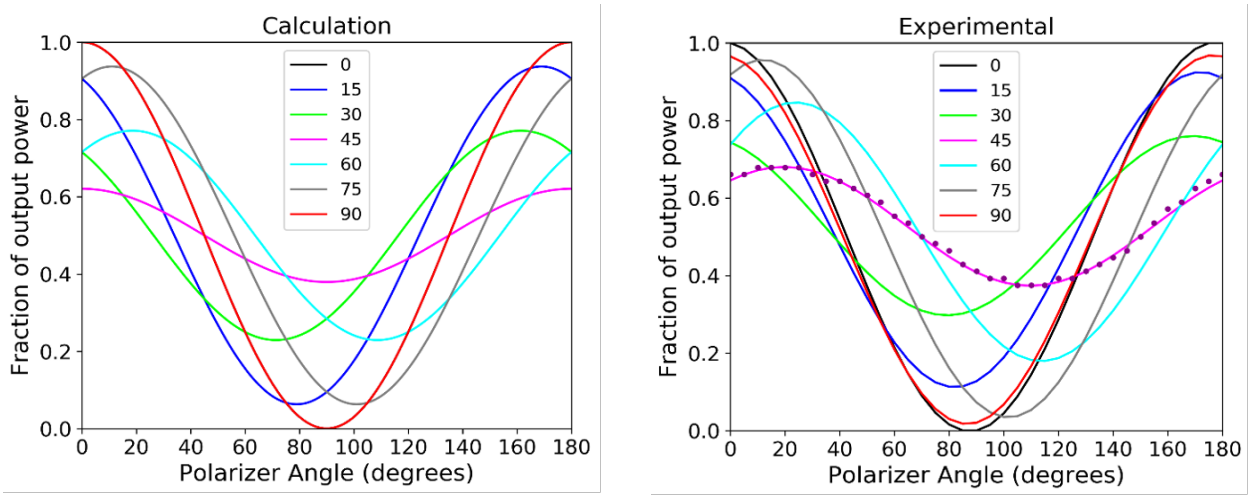

Figure 2: Ellipticity (a) calculation and (b) measurement (shown as a fit of the experimental data; representative data seen as points on the magenta, 45 degree measurement) of light after passing through different angles of the ZnO crystal. When the curve ranges from 0 to 1, the polarization is linear. Smaller ranges correspond to a more elliptical light. Therefore, when the crystal orientation is at 0 or 90 degrees, the output light is linear; when the crystal is at 45 degrees, the light is the most elliptical. Note that the 0 degrees of ZnO is exactly the same as 90 degrees, and thus only 90 degrees is visible in (a).

THE PEGASUS REVIEW:
UNIVERSITY OF CENTRAL FLORIDA
UNDERGRADUATE RESEARCH JOURNAL

URJ

13.1: 11-19

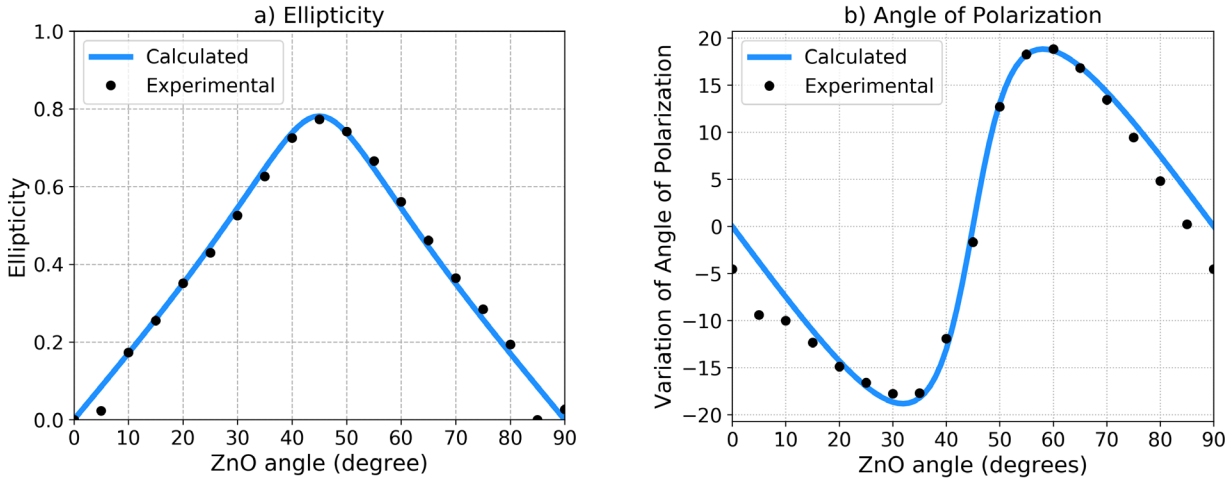

Figure 3. Changes in polarization as a function of ZnO angle. a) The largest ellipticity changes occur at 45 degrees, becoming near 0.8. Conversely, at 0 or 90 degrees there is no polarization change from passing through ZnO. b) The angle of polarization changes with the changing ZnO.

Overall, the ZnO meaningfully altered the inputted vertical polarization, and the agreement between the experimental and calculated results confirm the representation of ZnO as an arbitrary wave plate.

The half wave plate and quarter wave plate were then added to the setup in front of the ZnO crystal. The calculated output ellipticity for all possible configurations are summarized in Figure 4. Minima on the graph correspond to more linear polarization, or smaller ellipticity, and thus indicated the potential angle combinations for the setup. The shape of the minima depends on the phase delay caused by the crystal and the wavelength of the experiment, which in turn affects the index of refraction. Thus, this graph changes for crystals of different thicknesses and different crystals. The symmetry of the wave plates can be seen in the repetition of the pattern, where the quarter wave plate repeats twice every 180 degrees, while the half wave plate repeats four times every 180 degrees. This repetition is an expected characteristic of the wave plates and corroborates the validity of the calculations.

With these three optical elements, there is always a set of angles for each element that results in zero ellipticity. However, because our calculations were performed on a grid, we could not always find this 'perfect' combination of angles. Therefore, we selected the angle combinations with ellipticity less than 0.0125, which we considered to be effectively linear. Different crystal angles affected the number of possible angle configurations that gave linearly polarized light. For example, the ZnO crystal at angles of 40 and 50 degrees resulted in ellipticities close to 0.0125 with only a few possible configurations. Conversely, there were many options for configurations when the ZnO crystal was at 0 or 90 degrees, with several possible configurations resulting in ellipticities on the order of 10^{-3} or smaller. These points are marked in red in Figure 4. The multiple options for angles can be explained by the symmetry of the wave plates, where the system repeats every 90 degrees of both wave plates. Therefore, the locations of minima appear every 90 degrees. This symmetry allows for a choice in angle in the experimental setup. As the ZnO angle changed during rotational measurements, the location of minimum ellipticity changed; therefore, the half wave plate and quarter wave plate had to be rotated. Multiple angle options permitted moving each optic a smaller amount.

The polarization measurement was experimentally repeated with the wave plates at the calculated angles that gave linear, vertical polarization (Figure 5) to confirm that the calculated angles worked experimentally. An example of one potential setup of angles is given in Table 1. These angles were chosen from multiple possible angle combinations, as seen in Figure 4. The location of the minima at 90 degrees shows that this polarization is vertical and the range from 0 to 1 indicates that the polarization is linear, as desired. For crystal orientations near 45 degrees and 135 degrees, the ellipticity does not

THE PEGASUS REVIEW:
UNIVERSITY OF CENTRAL FLORIDA
UNDERGRADUATE RESEARCH JOURNAL

URJ

13.1: 11-19

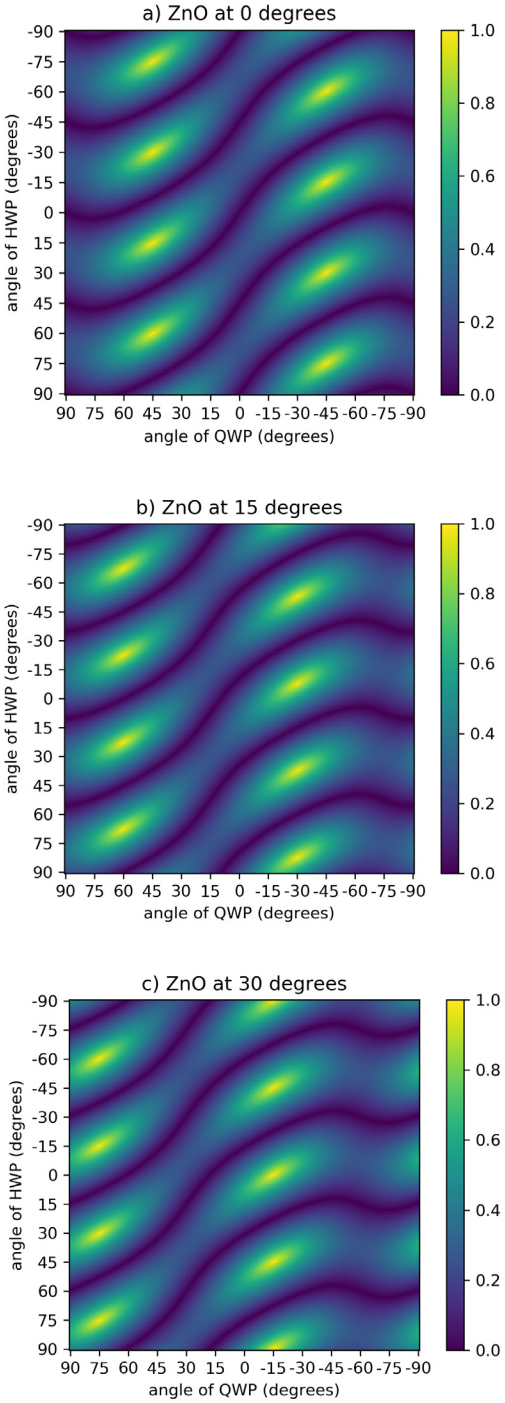

Figure 4: Ellipticity measurements for ZnO angle of a) 0 degrees, b) 15 degrees, and c) 30 degrees showing corresponding angles of the HWP and QWP. Red points in a) mark the location of vertical polarization with ellipticity less than 0.0125.

quite reach zero transmitted power, showing that we do not achieve perfectly linear polarization. This ellipticity may introduce error in later measurements, but this polarization is much closer to a linear, vertical polarization than what is found without the wave plates' correction, as the angles of 45 and 135 degrees experience the most polarization change from ZnO (described earlier in Figure 3). Therefore, our results confirm that a Jones calculus technique of using wave plates to counteract the effect of the ZnO on the polarization is experimentally feasible.

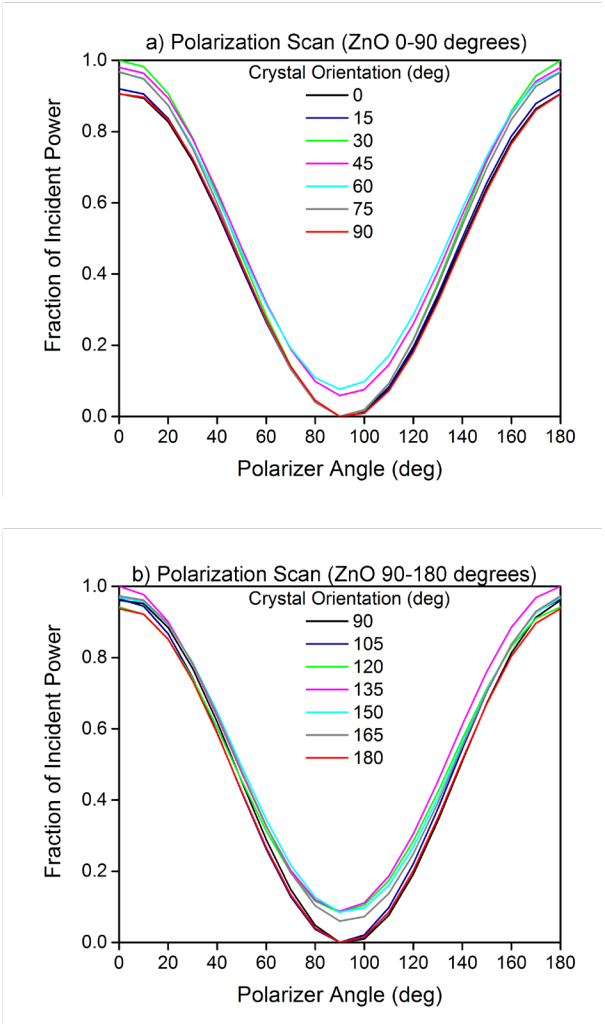

Figure 5. Polarization scan after using calculated angles for the setup. Vertical, linear polarization is achieved for crystal orientations from (a) 0 to 90 degrees and (b) 90 to 180 degrees. In comparison with Figure 2a, the polarization states are much more uniform and close to linear polarization (red curve in Figure 2a for all crystal orientations).

THE PEGASUS REVIEW:
UNIVERSITY OF CENTRAL FLORIDA
UNDERGRADUATE RESEARCH JOURNAL

URJ

13.1: 11-19

ZnO	QWP	HWP
0	0	0
5	8	6
10	15	12
15	23	18
20	31	24
25	41	31
30	50	37
35	62	45
40	76	53
45	90	60

Table 1. Potential configuration of angles

An angle-dependent HHG spectrum was taken with this linear polarization. Figure 6 compares the HHG spectrum from only bulk ZnO to the new setup with the calculated angle configurations of each component. Figure 6a shows harmonic signal with the calculated HWP and QWP angles for each ZnO angle, while Figure 6b shows the harmonic signal from ZnO with no corrections to polarization. In other words, Figure 6a shows the harmonics generated with nearly linear polarization at the exit of the crystal, while Figure 6b shows the harmonics from variable elliptical polarization resulting from propagation through the crystal.

The orientation-dependent harmonic spectra in Figure 6a and 6b share some general features. For example, in both cases we can observe odd and even harmonic orders when the driving laser is polarized along the c-axis (0 degrees) and only odd harmonics for polarization perpendicular to the c-axis (90 degrees), in accordance with symmetry considerations. However, there are also significant differences between the two sets of spectra. In Figure 6b, weak maxima in the even harmonic yield are observed for angles between 60 and 75 degrees, features which are absent from the polarization-corrected data in Figure 6a. Instead, the polarization-corrected data shows additional maxima of both odd and even harmonics for a crystal orientation of approximately 35 degrees. These differences require further study, such as comparison with reflection geometry, which does not display the propagation effects we are attempting to counteract with Jones calculus. Additionally, more theoretical study of the HHG process in solids, such as through DFT calculations, may be able to explain the observed polarization dependences. We note that explaining the orientation-dependent spectrum of HHG in ZnO is an active area of research at this time, and no theory has yet been able to fully reproduce the experimentally-observed behavior[25,26].

The mid-IR wave plates may have introduced errors in the polarization-corrected data. We chose to use low-order wave plates designed for operation at 3500 nm, as they had relatively low cost, high transmission (>95% over the spectral bandwidth of the laser) and used a MgF_2 substrate, which is less susceptible to nonlinear propagation than Si substrates. However, the relatively larger retardance (3/4 waves and 3/2 waves) and non-uniform retardance over the spectral bandwidth unintentionally lengthen the laser pulses and decrease its peak intensity. The reduced laser intensity weakens the high-order harmonic signal, resulting in a lower signal-to-noise ratio of the measurements using the wave plates.

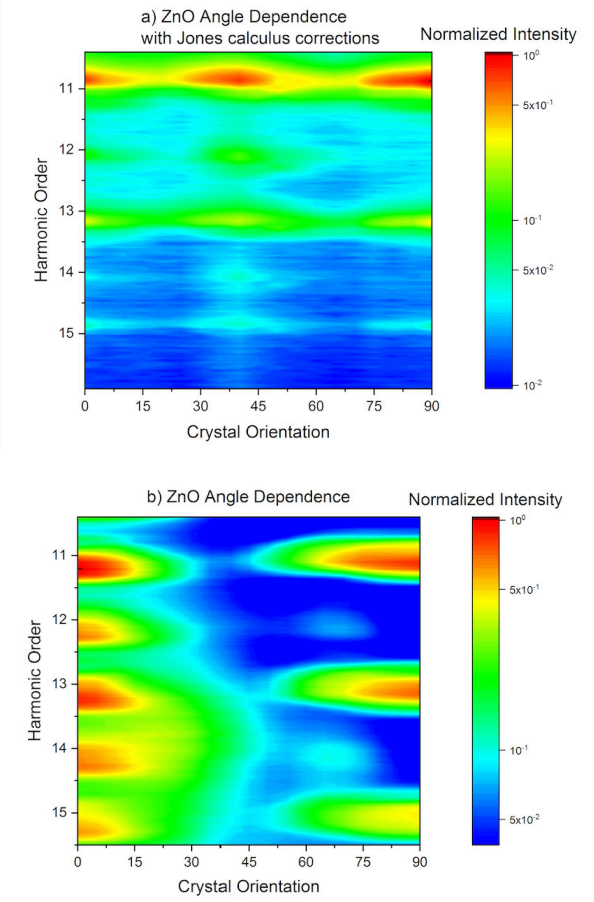

Figure 6: Experimental HHG spectra shown with a logarithmic intensity scale. a) HHG spectrum from the waveplates and ZnO at calculated angles. b) HHG spectrum from only bulk ZnO.

THE PEGASUS REVIEW:
UNIVERSITY OF CENTRAL FLORIDA
UNDERGRADUATE RESEARCH JOURNAL

URJ

13.1: 11-19

CONCLUSION

We show here that the propagation effects associated with HHG in bulk birefringent crystals can be accounted for using Jones calculus. Using this method, we are able to control the polarization at the exit of the crystal with the addition of a half wave plate and quarter wave plate to the system. We are thus able to 'choose' linear polarization at the end of the crystal by adjusting the angle of each wave plate and the crystal. We find changes in the angle dependent features by comparing the harmonic spectrum from linearly polarized light in bulk crystal to the harmonic spectrum from arbitrary polarization. The features are of interest to further study, as they give insight into the generation process and polarization dependence. This Jones calculus analysis allows us to better control and analyze the harmonic signal by accounting for the polarization change that occurs within bulk crystal, as the crystal can modify the polarization state an unknown amount without these corrections. This technique can be applied to other crystals as well, making Jones calculus an approachable way to increase confidence in bulk crystal HHG measurements.

ACKOWLEDGEMENTS

This work is supported by the Air Force Office of Scientific Research under award no. FA9550-16-1-0149, the National Science Foundation under grant nos. 1806135 and 1809181, and the UCF OUR Summer Undergraduate Research Fellowship.

THE PEGASUS REVIEW:
UNIVERSITY OF CENTRAL FLORIDA
UNDERGRADUATE RESEARCH JOURNAL

URJ

13.1: 11-19

WORKS CITED

[1]T. Popmintchev, M.-C. Chen, P. Arpin, M. M. Murnane and H. C. Kapteyn, Nature Photonics (2010).

[2]M. Garg, M. Zhan, T. T. Luu, H. Lakhotia, T. Klostermann, A. Guggenmos, and E. Goulielmakis, Nature **538** (7625), 359-63 (2016).

[3]S. Baker, J. S. Robinson, C. A. Haworth, H. Teng, R. A. Smith, C. C. Chirila, M. Lein, J. W. G. Tisch, and J. P. Marangos, Science **312** (2006).

4. M. Hohenleutner, F. Langer, O. Schubert, M. Knorr, U. Huttner, S. W. Koch, M. Kira, and R. Huber, Nature **523** (7562), 572-75 (2015).

[5]M. Drescher, M. Hentschel, R. Kienberger, M. Uiberacker, V. Yakovlev, A. Scrinzi, T. Westerwalbesloh, U. Kleineberg, U. Heinzmann, and F. Krausz, Nature **419** (2002).

[6]E. Goulielmakis, Z.-H. Loh, A. Wirth, R. Santra, N. Rohringer, V. S. Yakovlev, S. Zherebtsov, T. Pfeifer, A. M. Azzeer, M. F. Kling, S. R. Leone and F. Krausz, Nature **466**, (2010).

[7]T. T. Luu, M. Garg, S. Y. Kruchinin, A. Moulet, M. T. Hassan, and E. Goulielmakis, Nature **521** (7553), 498-502 (2015).

[8]S. Ghimire, A. D. DiChiara, E. Sistrunk, P. Agostini, L. F. DiMauro, and D. A. Reis, Nature Physics **7** (2), 138-41 (2010).

[9]G. Vampa, T. J. Hammond, N. Thire, B. E. Schmidt, F. Legare, C. R. McDonald, T. Brabec, D. D. Klug, and P. B. Corkum, Phys Rev Lett **115** (19), 193603 (2015).

[10]S. Eich, A. Stange, A. V. Carr, J. Urbancic, T. Popmintchev, M. Wiesenmayer, K. Jansen, A. Ruffing, S. Jakobs, T. Rohwer, S. Hellmann, C. Chen, P. Matyba, L. Kipp, K. Rossnagel, M. Bauer, M. M. Murnane, H. C. Kapteyn, S. Mathias, and M. Aeschlimann, J. Electron Spectrosc. & Relat. Phenom. **195**, 231-36 (2014).

[11]S. Ghimire, A. D. DiChiara, E. Sistrunk, G. Ndabashimiye, U. B. Szafruga, A. Mohammad, P. Agostini, L. F. DiMauro, and D. A. Reis, Phys Rev A **85** (4), (2012).

[12]S. Gholam-Mirzaei, J. Beetar, and M. Chini, Appl. Phys. Lett. **110**, (2017).

[13]S. Jiang, H. Wei, J. Chen, C. Yu, R. Lu, and C. D. Lin, Phys Rev A **96** (5), (2017).

[14]K. S. Budil, P. Salieres, M. D. Perry, and A. L'Huillier, Phys Rev A **48** (5), R3437-440 (1993).

[15]N. Dudovich, J. Levesque, O. Smirnova, D. Zeidler, D. Comtois, M. Y. Ivanov, D. M. Villeneuve, and P. B. Corkum, Phys Rev Lett **97** (25), 253903 (2006).

[16]D. Oron, Y. Silberberg, N. Dudovich, and D. M. Villeneuve, Phys Rev A **72** (6), (2006).

[17]N. Saito, P. Xia, F. Lu, T. Kanai, J. Itatani, and N. Ishii, Optica **4** (11), (2017).

[18]Y. S. You, David A. Reis, and S. Ghimire, Nature Physics **13** (4), 345-49 (2016).

[19]C. Liu, Y. Zheng, Z. Zeng, and R. Li, Phys Rev A **93**, (2016).

[20]N. Tancogne-Dejean, O. D. Mücke, F. X. Kärtner, and A. Rubio, Nature Communications (2017).

[21]P. Y. Xia, C. Kim, F. M. Lu, T. Kanai, H. Akiyama, J. Itatani, and N. Ishii, Opt Express **26** (22), 29393-9400 (2018).

[22]G. Vampa, Y. S. You, H. Liu, S. Ghimire, and D. A. Reis, Opt Express **26** (9), (2018).

[23]J. Peatross and M. Ware, *Physics of Light and Optics,* 2015 Edition ed. (Brigham Young University, 2017).

[24]W. L. Bond, J. Appl. Phys. **36** (5), 1674-677 (1965).

[25]S. Jiang, J. Chen, H. Wei, C. Yu, R. Lu, and C. D. Lin, Phys Rev Lett **120** (25), 253201 (2018).

[26]S. Jiang, S. Gholam-Mirzaei, E. Crites, J. E. Beetar, M. Singh, R. Lu, M. Chini, and C. D. Lin, J. Phys. B: At. Mol. Opt. Phys. **52** (2019).